Environmental Science Advances

ROYAL SOCIETY OF CHEMISTRY

PAPER

View Article Online
View Journal | View Issue

Cite this: *Environ. Sci.: Adv.*, 2026, **5**, 1039

Metastatic impact of perfluorooctanoic acid on liver cancer: insights from HepG2 cells and zebrafish xenograft models

Kayla E. Hawn,[a] Emma Kenyon,[a] Gregory Buck[a] and Wei Xu *[b]

Widely used in consumer products for its water- and grease-resistant properties, perfluorooctanoic acid (PFOA), a legacy per- and polyfluoroalkyl substance (PFAS), has been increasingly implicated in liver carcinogenesis. Long-term or high-level PFAS exposures have been found to be associated with an increased incidence of several types of cancers, including liver, kidney, and breast cancers. Despite mounting evidence linking PFAS exposure to hepatotoxicity and cancer, experimental models that enable real-time visualization of PFOA-induced carcinogenicity remain limited. To address this gap, we aimed to develop a liver tumor xenograft model using zebrafish (*Danio rerio*) embryos for the investigation of the carcinogenic effects of PFOA on human liver cells. To create the xenograft model with zebrafish embryos, human hepatic HepG2 cells were labeled with living cell imaging dyes and engrafted into fish embryos at one day post-fertilization. The embryos were then exposed to PFOA at concentrations of 0.1, 1.0, and 10 ppm for 24–96 hours. The *in vivo* cell proliferation was confirmed by quantifying the expression levels of a HepG2 housekeeping gene, hypoxanthine-guanine phosphoribosyltransferase 1 (hprt1). The expression profiles of two metastasis markers, *cdh1* and *mmp9*, suggested the induction of HepG2 cell metastasis by PFOA. The PFOA-triggered metastatic changes in HepG2 cells were also confirmed by the observation of cell migration inside the zebrafish embryos. Two polycyclic aromatic hydrocarbon (PAH) chemicals, anthracene and naphthalene (0.1–1.0 ppm), were used as both of them were reported to damage hepatic cells through activating the aryl hydrocarbon receptor (AhR) pathway. Although both PAH compounds altered the expression patterns of *cdh1* and *mmp9* in HepG2 cells, their capabilities to enhance the HepG2 proliferation *in vivo* were less significant compared to PFOA. The results demonstrated that prolonged chemical exposure to PFOA can promote HepG2 cell survival, proliferation, and metastasis *in vivo*. This zebrafish xenograft model provides a dependable and robust platform for mechanistic toxicology studies and is a mid-to high-throughput screening tool for environmental carcinogens and anti-cancer drug selection.

Received 24th December 2025
Accepted 22nd February 2026

DOI: 10.1039/d5va00491h

rsc.li/esadvances

Environmental significance

Widely detected in ecosystems and human tissues, the persistent per- and polyfluoroalkyl substances (PFASs) have been raising concerns about their carcinogenic potential. Efforts have been made to detect and mitigate PFASs in the environment; however, the assessment of the carcinogenic effects of the substances is limited. Using a zebrafish xenograft model with human HepG2 cells, we demonstrated that perfluorooctanoic acid (PFOA), one of the most common PFAS compounds, enhanced tumor cell proliferation, migration, and metastatic marker expression. Mechanistic investigation indicated activation of the aryl hydrocarbon receptor (AhR) pathway, likely *via* crosstalk with peroxisome proliferator-activated receptor (PPAR) signaling. This work provides direct insight into PFAS-driven hepatocellular carcinoma progression and introduces a rapid, high-throughput platform for assessing environmental carcinogens.

Introduction

Per- and polyfluoroalkyl substances (PFASs) are prominent synthetic materials used in everyday items such as fire retardants, water-resistant materials, non-stick cooking products, and food packaging. One PFAS, per-fluorooctanoic acid (PFOA), is listed as one of the most abundant priority pollutants by the United States Environmental Protection Agency (EPA) and it is estimated that 700 tons are emitted world-wide annually.[1] PFOAs have a half-life of 2.3–8.5 y after being absorbed by humans through inhalation, dermal contact and water consumption leading to bioaccumulation in the liver, kidneys, and serum.[2] Once absorbed, these exogenous

[a]*Department of Life Sciences, Texas A&M University – Corpus Christi, Corpus Christi, TX 78412, USA*

[b]*Department of Veterinary Physiology & Pharmacology, Texas A&M University College of Veterinary & Biomedical Sciences, College Station, TX 77843, USA. E-mail: wxu1@tamu.edu*

compounds interfere with endocrine functions thus inciting hormone dysregulation, altering metabolic pathways (such as CYP) and increasing oxidative stress.[3] The potential carcinogenicity of these endogenous chemicals creates a greater need for understanding their function and mechanism in humans.

Liver cancer remains a significant global health challenge, with hepatocellular carcinoma (HCC) representing the most prevalent form of primary liver cancer, accounting for approximately 90% of cases.[4] It is the fifth most common cancer worldwide and ranks as the second leading cause of cancer related deaths.[5,6] HCC arises from malignant transformation of hepatocytes and is marked by the development of abnormal arterial-like vessels that become more prominent, increasing vascular permeability as the disease progresses, and lead to blood oxygenation instability and aggressive tumor progression when coupled with the loss of pericytes.[7] While curative treatments are highly effective in early stages, advanced stage tumors are unresectable and reduce survivability to about five months due to cancer's resistance to chemotherapy and radiation.[8,9] The prognosis of HCC is a five-year survival rate ranging between 10% and 30%, with a mortality rate expected to increase by 55% by 2040.[10,11] Western countries have experienced a threefold increase in HCC over the past four decades, likely driven by the hepatitis C virus, obesity, and prolonged exposure to environmental toxins, such as perfluorooctanoic acid (PFOA) and polycyclic aromatic hydrocarbons (PAHs).[12,13] These trends highlight the urgent need for improved molecular models and innovative therapies to enhance patient outcomes.

Zebrafish (*Danio rerio*) are increasingly recognized as a versatile *in vivo* model species for studying human-derived xenografts using human tumor cells for assessing tumorigenesis. Unlike traditional murine models, which often require months for complete organogenesis, observable tumor growth, toxicological responses, and immunosuppression, zebrafish rapidly develop and reproduce for streamlined high-throughput models optimal for experimental workflows. Approximately 70% of human genes have zebrafish orthologs, including cytochrome P450 (CYP) genes, suggesting conserved signaling pathways exist for translational relevance for drug response and carcinogenesis studies.[14–16] Further enhancing their utility, zebrafish lack innate immunity until ~7 days post fertilization (dpf) and adaptive immunity until ~27 dpf, permitting the successful engraftment of human cancer cells in patient derived xenograft (PDX) models.[17] This lack of hindrance by immune cells has been modeled by the successful cancer cell engraftment into zebrafish embryos at 2 dpf.[18,19] Monitoring real time progression of cancer cells is also attainable using fluorescence microscopy due to zebrafish melanophores not being developed until 14 dpf, thus resulting in transparent embryonic and larval bodies.[15] Lastly, the liver is essential for oxidation, reduction, and hydrolysis mediated by CYP, which is responsible for phase I and phase II metabolism of endogenous compounds. As such, the development of the liver in zebrafish and the specification by transcription factor function shared with humans are expressed within the first week of development, making them ideal species for modeling liver diseases.[15]

In this study, we developed a human hepatocellular cancer cell zebrafish xenograft model to better characterize the carcinogenic effects of PFOA on hepatocellular carcinoma, examining the proliferation and metastasis of HepG2 cells *in vivo* and testing the capability of PFOA to induce the AhR pathway, influencing carcinogenic potential. Since chemicals with aromatic rings are typically considered potential ligands for AhR, we also applied two polycyclic aromatic hydrocarbon compounds, anthracene and naphthalene, as the positive controls for this study.

Experimental

HepG2 cell line and zebrafish

All experimentation on zebrafish was performed in compliance with the Texas A&M University institutional guidelines and approved by the Institutional Animal Care and Use Committee (TAMU-CC-IACUC-2023-0015) and the Institutional Biosafety Committee (TAMU-CC-IBC-2023-0003). Zebrafish were bred and raised within aquarium systems at Texas A&M University – Corpus Christi. Human cell line HepG2-Lucia™ AhR cells (InvivoGen, San Diego, CA) contained an AhR luciferase reporting system and were a generous gift from Dr Ramon Lavado at Baylor University. Cells were cultured in Dulbecco's modified essential medium (DMEM, Corning Inc., Corning, New York) supplemented with 10% fetal bovine serum (FBS, VWR International LLC., Radnor, PA), 100 μg mL^{-1} of penicillin and 100 μg mL^{-1} of streptomycin (Invitrogen Co., Waltham, MA) at 37 °C and 5% CO_2 input.

HepG2 cell engraftment into zebrafish embryos

HepG2-Lucia™ AhR cells were harvested, thoroughly washed and resuspended with PBS, and quantified using a hemacytometer. The cell density was adjusted to 10^8 cells per mL with PBS. One hundred microliters of cell suspension was aliquoted to a new tube and labelled with a Qtracker™ 625 Cell Labelling Kit (Invitrogen Co.) following the manufacturer's instructions. The prestained cells were then collected, washed, and resuspended with PBS to a density of 5×10^5 cells per μL. The cell suspension in PBS was backfilled into the microinjector needle with Eppendorf Femtotips™ Microloader Tips (Eppendorf North America, Enfield, CT). Zebrafish embryos at 24 hours post fertilization (hpf) were anesthetized with $NaHCO_3$-buffered tricaine methanesulfonate (MS-222, 150 mg L^{-1}, pH 7.0, Sigma-Aldrich Co., St. Louis, MO). The engraftment of the cells into zebrafish embryos was performed with a WPI pneumatic microinjection system (World Precision Instruments, Sarasota, FL). One nanoliter of cell suspension was injected into the yolk of each zebrafish embryo to engraft 500 cells per embryo. The embryos containing HepG2-Lucia™ AhR cells were immediately moved to freshly filtered zebrafish aquarium water after microinjection and incubated at 30 °C. The temperature was gradually increased to 36 °C (+1 °C per day) to optimize human cell growth. Neither temperature increase nor the injection method altered zebrafish survivability based on our previous studies.[18,19]

Assessment of HepG2 cell metastasis *in vivo*

The levels of HepG2 cell metastasis were estimated by cell migration, proliferation, and metastatic marker gene expression *in vivo*. Fluorescently labelled HepG2-Lucia™ cells engrafted into zebrafish embryos were visualized daily using an Olympus CKX53 inverted microscope equipped with a U-HGLGPS fluorescence light source (Olympus, Japan). The number of HepG2 cells in zebrafish embryos (before hatching) and larvae (after hatching) was estimated with the quantitative PCR (qPCR) method previously developed in our lab.[18,19] Briefly, zebrafish embryos/larvae without engraft were collected daily from 2 to 8 dpf. HepG2-Lucia™ cells were harvested and resuspended in PBS. Each zebrafish embryo or larva was mixed with a known number of HepG2-Lucia™ cells to make a sample (*i.e.*, 1 embryo at 1 dpf mixed with 500 cells, 1 embryo at 1 dpf mixed with 5000 cells, 1 embryo at 2 dpf mixed with 500 cells, *etc.*). The number of HepG2-Lucia™ cells in each sample was 50, 500, 5000, or 50 000. Each sample, containing an embryo/larva and a certain number of cells, was mixed with 1 mL TRIzol reagent (Molecular Research Center, OH, USA) and 100 μL glass beads (2 mm diameter), followed by homogenization with a Precellys® 24 Touch tissue homogenizer (Bertin Technologies, Montigny-le-Bretonneux, France).

The total RNA of each sample was isolated following the standard procedure of the TRIzol method, and the DNA in each RNA sample was removed using the TURBO DNA-free™ Kit (Invitrogen Co.). The amount of RNA in each sample was measured with a Eppendorf BioPhotometer D30 Model 6133 (Eppendorf North America). Approximately 200 ng RNA from each sample was used for cDNA synthesis using the SuperScript IV Reverse Transcriptase single-stranded cDNA synthesis kit (Invitrogen Co.) combined with a random hexamer primer (synthesized by Integrated DNA Technologies, Coralville, IA). The qPCR was performed with the cDNAs using the SYBR Green method on a QuantStudio™ 5 Real-Time PCR thermocycler (Applied Biosystems, Waltham, MA). The corresponding qPCR cycle threshold (C_t) values of the human housekeeping genes, encoding TATA-binding protein (TBP) and hypoxanthine-guanine phosphoribosyltransferase 1 (HPRT1), were plotted against the log10 of cell counts, establishing a standard curve to reference for each life stage, according to prior modeling.[18,19] The primers used for these two genes were previously proven to be human-specific with no non-specific amplifications from zebrafish cDNAs (SI Table S1). An equation of linear regression was generated from the standard curve.

Zebrafish embryos and larvae with the HepG2-Lucia™ cell engraft were also collected and humanized for total RNA extraction following the same procedure as used in the preparation of the standard curve. Two hundred nanograms of RNA from each sample were used for cDNA synthesis and qPCR to generate the corresponding C_t values following the same methods for standard curve generation. The C_t value of each sample was used to calculate the number of HepG2-Lucia™ cells *in vivo* with the regression equation of the standard curve.

In addition, the metastatic status of the HepG2-Lucia™ cells *in vivo* in response to the chemical treatments was evaluated by measuring the transcript levels of two metastatic marker genes, encoding *E*-cadherin-1 (CDH1) and matrix metalloproteinase-9 (MMP9). Similarly, RNAs were isolated from the embryos and larvae carrying the HepG2-Lucia™ AhR cells. The RNA isolation, cDNA synthesis, and qPCR were performed following the procedures described above.

Activation of AhR HepG2 cells by environmental pollutants

HepG2-Lucia cells with activated AhR were cultured in 96-well plates and exposed to various chemicals, including anthracene, naphthalene, and PFOA, at concentrations of 0.1, 1, or 10 ppm. Anthracene and naphthalene are known as AhR ligands, while PFOA is reported to be an AhR activator previously (Larson *et al.*, 2018). Due to the low solubilities in water, all chemicals were first dissolved in DMSO and diluted with cell culture media for the treatment. Therefore, DMSO diluted with cell culture media was used as a control. Treated cells were incubated for two hours. Twenty microliters of media from each well were collected and applied to the detection of luciferase activities using the Quanti-Luc 4 Lucia/Guassia glow detection kit (InvivoGen). The luminescence of each well was then read using a Cytation™ 5 microplate reader (BioTek) within 30 min from the start of the reaction.

In vivo activation of HepG2 cells by environmental pollutants

The fish embryos transplanted with HepG2-Lucia™ AhR cells were incubated at 28 °C for 24 hours in a 96-well plate with a density of one embryo per well. Chemicals were then diluted in molecular-grade water immediately prior to zebrafish trials. Based on the *in vitro* luciferase activation results, zebrafish were treated with naphthalene or PFOA at concentrations of 0.1 ppm and 1.0 ppm and PFOA at 0.1 ppm, 1.0 ppm and 10 ppm. Molecular-grade water was used as a control for luciferase activity measurements. Six trials with 42 embryos each were used for the assessment of AhR activation *in vivo*. Each HepG2-Lucia™ AhR cell-engrafted embryo was incubated for 3 days post injection (dpi) before chemical treatments were administered. On the day of chemical treatment, filtered zebrafish water was drained from each well and replaced with 150 μL prepared treatments, including seven embryos with molecular water as control and five embryos with each concentration of anthracene (0.1 ppm and 1.0 ppm), naphthalene (0.1 and 1.0 ppm), and PFOA (0.1, 1.0, and 10 ppm). During the treatment, 20 μL of supernatant was collected from each well at 24 and 48 hours post treatment (hpt) for detection of luciferase activities according to the Quanti-Luc 4 Lucia/Guassia kit.

Statistical analyses

First, the Shapiro–Wilk test[20] was applied to all the data to determine if the data generated from the qPCR or Luciferase assay followed the normal distribution. The dataset with the normal distribution was analyzed using one-way analysis of variance (ANOVA) followed by *post hoc* testing (TukeyHSD). The non-normally distributed dataset was analyzed using the Kruskal–Wallis test[21] followed by Dunn's test for multiple comparisons.[22] Adjusted *p*-values generated from the statistical analyses

were used to detect significant differences between groups. All the results of data normality analysis were included in the SI (Fig. S1–S3).

Results and discussion

Establishing the HepG2 xenograft model

As a protocol developed from our previous studies,[18,19] we injected the HepG2-Lucia™ AhR cells into the zebrafish embryo at 24 hpf and performed daily observation until 6 dpf (Fig. 1a). The location of microinjection was close to the cardiac chamber of the fish embryo (Fig. 1b) and remained consistent in all injected embryos. The migration of HepG2-Lucia™ AhR cells was observed as early as 24 hours post injection (1 dpi, Fig. 1c), although the majority of the injected cells were found around the yolk. A small number of cells were absorbed near the middle section of the body and no cells were found near the caudal fin or the posterior section of the trunk (Fig. 1c). In comparison, more HepG2-Lucia™ AhR cells were found in the middle to rear sections of the fish embryo at 3 dpi. HepG2-Lucia™ AhR cells were also observed in the cardiac chamber of the larva at 3 dpi (Fig. 1d). At 5 dpi, HepG2-Lucia™ AhR cells were identified near the eyes and dorsal area of the larva, as well as the different trunk sections (Fig. 1e). Although fluorescence imaging showed direct evidence of cell migration *in vivo*, it was difficult to estimate the number of cells inside the fish embryos/larvae. Therefore, we applied a qPCR assay for the quantification of HepG2-Lucia™ AhR cells in fish embryos/larvae.[18,19] The idea was to specifically measure the transcript levels of human cell housekeeping genes. In this study, we used the primers that were previously designed and have been proven to be specific to human cells.[19] No zebrafish transcripts were amplified when the qPCRs with these primers were applied to the mixture of human and zebrafish cDNAs.[19] We generated two standard curves with two pairs of human housekeeping gene-specific primers. The cDNA template for each qPCR reaction was generated with a pool of RNAs from a zebrafish embryo/larva at a certain developmental stage (2, 3, 4, 6, 7, or 8 dpf) and a known number of HepG2-Lucia™ AhR cells (50, 500, 5000, or 50 000). The C_t value (X-axis) generated from each reaction was used to construct the standard curve against the log10 of the cell number (Y-axis). For the *tbp* gene, we generated a standard curve with a regression $y = -2.2158x + 84.927$, where y is the log10 of the HepG2-Lucia™ AhR cell number *in vivo* and x is the C_t value from the qPCR. The coefficient of determination (R^2) of the regression analysis is 0.6436 (SI Fig. S4). In contrast, the results from the *hprt1* gene quantification generated a standard curve, $y = -0.7797 + 31.583x$. The R^2 of this equation was 0.8776, which represented an improved regression compared to the equation from the *tbp* gene (Fig. 1f). Therefore, we used $y = -0.7797 + 31.583x$ to estimate the actual numbers of HepG2-Lucia™ AhR cells *in vivo*.

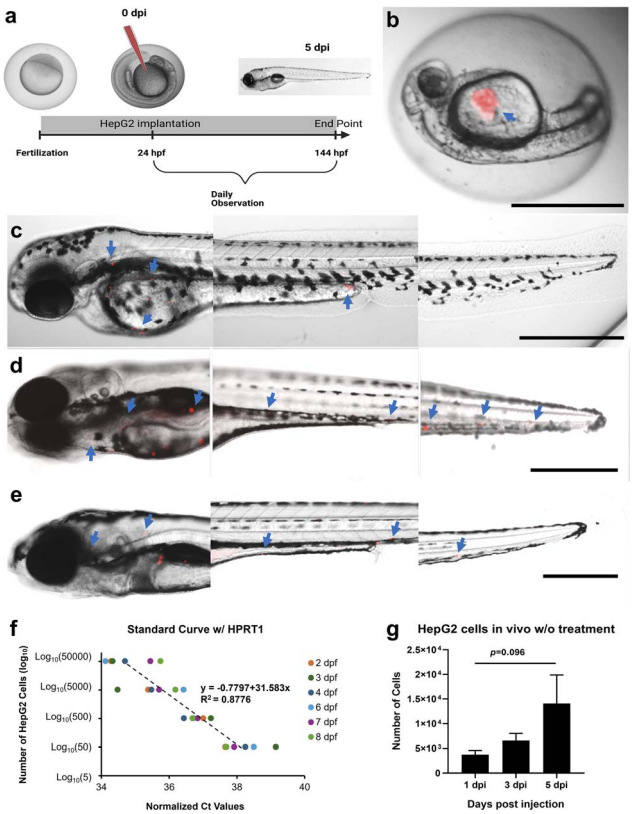

Fig. 1 Establishment of the HepG2 zebrafish xenograft model. The procedures for injection, monitoring, and sample collections are shown (a). Distributions of pre-labeled HepG2-Lucia™ AhR cells were observed at 0 (b), 1 (c), 3 (d), and 5 (e) dpi ($n = 10$). Scale bar: 200 μm, blue arrows: locations of HepG2 cells. The standard curve was generated by mixing various concentrations of HepG2-Lucia™ AhR cells with zebrafish embryos/larvae at different dpf. Log10-transformed cell numbers and qPCR C_t values of housekeeping gene *hprt1* for linear regression were determined using average values from all samples with the same number of HepG2-Lucia™ AhR cells (f, $n = 3$). The equation generated from the linear regression was used to estimate the actual numbers of *in vivo* HepG2-Lucia™ AhR cells in the embryos/larvae (g).

With the assistance of this standard curve, we first estimated the number of *in vivo* HepG2-Lucia™ AhR cells at different developmental stages. The number of cells rapidly increased from approximately 500/embryo (0 dpi) to 3768 ± 821 (mean ± sem) at 1 dpi, 6566 ± 1453 at 3 dpi, and 14 083 ± 5803 at 5 dpi (Fig. 1g). Although the increase in cell numbers from day 1 to day 5 post injection was not statistically significant, the increasing trend of the cell numbers suggested the active proliferation of HepG2-Lucia™ AhR cells inside the embryos or larvae.

It was noteworthy that the increase in *in vivo* HepG2-Lucia™ AhR cells was the most significant at 1 dpi, from 500 to over 3500 cells within 24 hours. This abrupt increase in human cells engrafted in zebrafish embryos was also observed in our previous studies. The number of prostate tumor cells was rapidly elevated from 5–6 (0 dpi) to over 30 (2 dpi) per larva on average.[19] Similarly, the breast cancer cells in zebrafish embryos expanded from ~200 cells per embryo (0 dpi) to over 1000 cells per larvae at 1 dpi.[18] One of the possible explanations was that most of the zebrafish embryos started hatching after 2 dpf. The nutrients and proteinous substances in the perivitelline fluid in

the chorion might provide support to the growth of the cancer cells *in vivo*.[23,24]

PFOA promotes HepG2 metastasis

PFOA was deemed a human carcinogen by the International Agency for Research on Cancer[25] and the Environmental Protection Agency[26] classified PFOA as likely to be a human carcinogen. Using the xenograft model in zebrafish with human cells and prolonged exposure to PFOA allowed real-time observation and estimation of carcinogenic effects from this compound. Following the characterization steps developed from the xenograft model establishment, we treated the zebrafish embryos 48 hours post HepG2-Lucia™ AhR cell injection (72 hpf) after they were hatched. The larval zebrafish were used for daily imaging as well as harvested for HepG2-Lucia™ AhR cell quantification (Fig. 2a). 24 hours of treatment with PFOA generally enhanced the migration of HepG2-Lucia™ AhR cells *in vivo* at all doses compared to the non-treated group (Fig. 2b). In particular, more HepG2-Lucia™ AhR cells were found surrounding the cardiac chamber and the eyes of the larvae in the 0.1 ppm treated group (Fig. 2c). The migration of HepG2-Lucia™ AhR cells appeared to be independent of the doses of the PFOA, since 1 ppm (Fig. 2d) and 10 ppm (Fig. 2e) PFOA treatment showed no significant difference in cell migration. In contrast, the proliferation of HepG2-Lucia™ AhR cells in larvae in response to the PFOA was found to be dose dependent. Although 0.1 and 1 ppm PFOA treatment increased the numbers of HepG2-Lucia™ AhR cells to 9561 ± 1284 and 8059 ± 2044, respectively, compared to the non-treated group (2732 ± 1011), there were no statistical differences ($p = 0.878$ for 0.1 ppm *vs.* non-treated; $p = 0.937$ for 1 ppm *vs.* non-treated). Only the 10 ppm treated group demonstrated a significant increase in the HepG2-Lucia™ AhR cell number (30 716 ± 12 705) compared to the non-treated group (*$p = 0.030$). The dose-independent pattern of the HepG2-Lucia™ AhR cell *in vitro* migration in response to PFOA might be attributed to the involvement of immune cells,[27] such as macrophages and neutrophils, which were developed in zebrafish embryos as early as 30 hpf.[28]

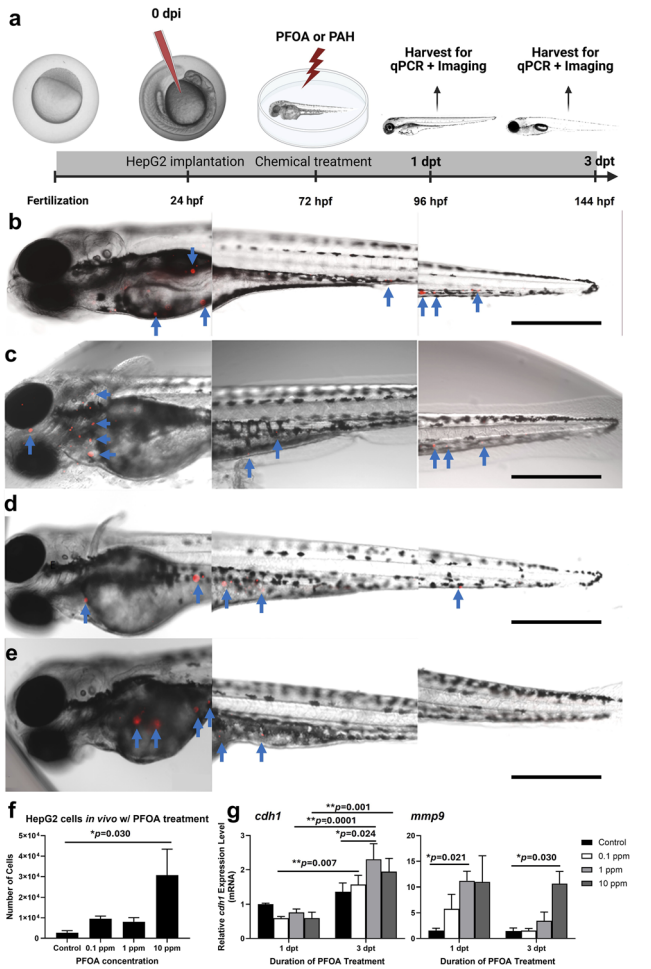

Fig. 2 *In vivo* development of HepG2-Lucia™ AhR cells in zebrafish larvae treated with PFOA. The procedures of the experiment including the timing of treatment are shown (a). Cell migration in zebrafish larvae was identified after 24 hours of treatment with 0 (b, control), 0.1 (c), 1 (d), and 10 (e) ppm PFOA (scale bar: 200 μm, blue arrows: locations of HepG2 cells). Proliferation of HepG2-Lucia™ AhR cells in zebrafish larvae at 24 hpt of PFOA was analyzed using qPCR on *hprt1* gene as described earlier (f, $n = 6$; $0.01 < *p < 0.05$). Expressions of two metastatic markers in HepG2 cells, *cdh1* and *mmp9*, were estimated by qPCR at 1 and 3 dpt of PFOA (g, $n = 4–8$; $**p < 0.01$).

The second cell metastatic marker, *mmp9*, demonstrated consistently upregulated expression patterns under the stress of PFOA after 1 and 3 days of treatment (Fig. 2g). Specifically, the 1 ppm PFOA treatment resulted in an 11.19 ± 1.86 fold increase of the control expression level (*$p = 0.021$) while 10 ppm PFOA treatment led to a 10.64 ± 2.38 fold *mmp9* expression over the control (*$p = 0.030$). The matrix metalloproteinase 9 enzyme was known to break down the extracellular matrix, enabling the migration of tumor cells,[34] including hepatocytes.[35,36] The consistent upregulation of mmp9 was associated with the

In addition, we also measured the transcription levels of two cell metastatic markers, *cdh1* and *mmp9*. Although current cellular mechanisms leading to hepatocellular carcinoma progression remain uncertain, recent studies have highlighted the utility of *E*-cadherin and matrix metalloproteinase 9 as metastatic biomarkers during epithelial–mesenchymal transition (EMT). Acting as a tumor suppressor, the *E*-cadherin's downregulation was found strongly linked to aggressive tumors including metastatic HCC.[29,30] The downregulation of *cdh1* was also observed after 24 hours post treatment (hpt), although no significant differences were found between control and any doses (Fig. 2g). Interestingly, the expression patterns of cdh1 were reversed at 3 days post treatment (dpt). Although there was still no significant difference between treatment groups and control (non-treated group), significant differences were found between 1 and 3 dpt in each dose (Fig. 2g). This type of expression pattern change in *cdh1* was commonly observed in the metastatic processes of many types of tumor cells, since the downregulation of *cdh1* expression promotes cell migration during EMT, while the upregulation of this cell junction protein contributes to the metastatic tumor formation in new locations.[31–33]

continuous migration of HepG2-Lucia™ AhR cells *in vivo* as observed by imaging.

Anthracene and naphthalene showed similar metastatic effects on HepG2 cells

As two common polycyclic aromatic hydrocarbon (PAH) compounds, anthracene and naphthalene are known to be the ligands for the aryl hydrocarbon receptor (AHR), the activation of which was strongly associated with the induction of several types of cancers, such as breast cancer,[37] lung cancer,[38,39] liver cancer,[40,41] prostate cancer,[42,43] ovary cancer,[44,45] glioma,[46] and skin cancer.[47–49] We also tested the metastatic effects of anthracene and naphthalene on the HepG2 cell zebrafish xenograft model, expecting to find if PFOA's carcinogenic effects were also *via* the AhR pathway. With the treatment protocols similar to that for the PFOA, we examined the migration of HepG2-Lucia™ AhR cells *in vivo* under the stress of anthracene and naphthalene.

Compared to the non-treated control larvae at 3 dpi (Fig. 3a), one day of anthracene treatment at both 0.1 (Fig. 3b) and 1 (Fig. 3c) ppm visibly promoted the HepG2-Lucia™ AhR cell proliferation *in vivo*; however, the overall migration patterns were different. As the majority of the HepG2-Lucia™ AhR cells migrated towards the posterior section in control larvae (Fig. 3a), more cells were found in the anterior side of the individuals treated with 0.1 ppm anthracene (Fig. 3b). One ppm anthracene treatment appeared to result in more HepG2-Lucia™ AhR cells *in vivo*; however, most of the cells were distributed in the yolk sac area (Fig. 3c). Indeed, the qPCR quantification confirmed the enhanced HepG2-Lucia™ AhR cells *in vivo* by anthracene treatment as they averaged 12 133 ± 3086 (*$p = 0.015$ compared to control) and 8338 ± 1500 ($p = 0.168$ compared to control) cells in the 0.1 and 1 ppm anthracene treated larvae, respectively, in comparison to 2732 ± 1011 cells in non-treated control larvae (Fig. 3d). We also found similar expression patterns of *cdh1* and *mmp9* in HepG2-Lucia™ AhR cells responding to anthracene treatment, down-regulation at 1 dpt and upregulation at 3 dpt for *cdh1* and consistent upregulation of *mmp9* with the treatment of both 0.1 and 1 ppm anthracene (Fig. 3e).

The treatment of anthracene showed a greater enhancement in promoting the HepG2-Lucia™ AhR cell migration *in vivo*. In comparison to the non-treated control larvae (Fig. 4a), the larvae treated with 0.1 ppm naphthalene showed fewer HepG2-Lucia™ AhR cells near the original injection site but much greater numbers in the middle and rear sections of the trunk (Fig. 4b). 1 ppm naphthalene appeared to drive the HepG2-Lucia™ AhR cells further down toward the caudal fins of larvae, as very few cells were found in the anterior and middle portion of the larvae (Fig. 4c). The cell numbers quantified with the qPCR showed an increase in the *in vivo* HepG2-Lucia™ AhR cell number when the embryos were treated with 0.1 ppm naphthalene (7721 ± 2661) compared to the non-treated control group (2732 ± 1011), although no statistically significant

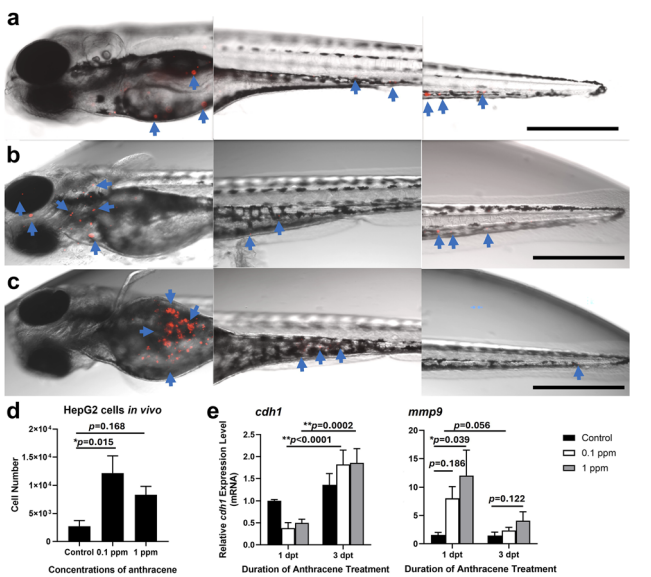

Fig. 3 Characterization of HepG2-Lucia™ AhR cells in zebrafish larvae treated with anthracene. HepG2-Lucia™ AhR cells were annotated in zebrafish larvae using fluorescence microscopy combined with image analysis after 24 hpt with 0 (a, control), 0.1 (b), and 1 (c) ppm anthracene (scale bar: 200 μm, blue arrows: locations of HepG2 cells). The number of HepG2-Lucia™ AhR cells in zebrafish larvae at 24 hpt of anthracene was measured using qPCR on the *hprt1* gene and the standard curve as described earlier (d, $n = 6$; $0.01 < *p < 0.05$). Expressions of metastatic markers, *cdh1* and *mmp9*, were quantified by qPCR at 1 and 3 dpt of anthracene (e, $n = 4–8$; $**p < 0.01$).

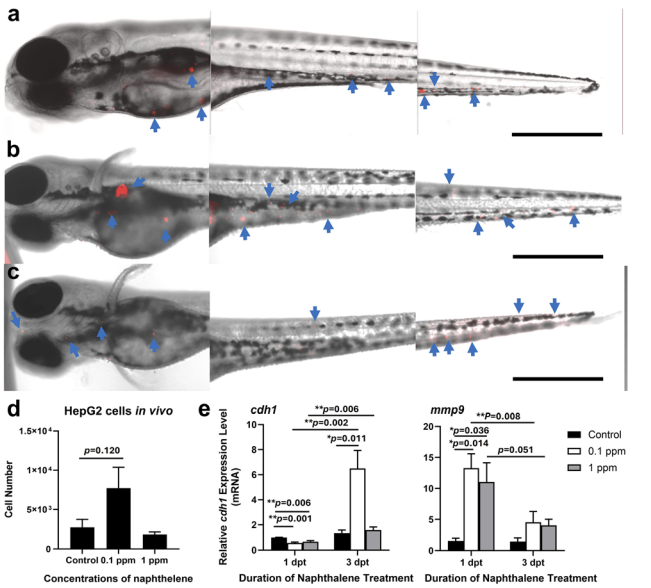

Fig. 4 Progression of HepG2-Lucia™ AhR cells in zebrafish larvae treated with naphthalene. The distributions of HepG2-Lucia™ AhR cells in zebrafish larvae after 24 hpt with 0 (a, control), 0.1 (b), and 1 (c) ppm naphthalene were observed using fluorescence microscopy and image analysis (scale bar: 200 μm, blue arrows: locations of HepG2 cells). The *in vivo* HepG2-Lucia™ AhR cells in zebrafish larvae at 24 hpt of naphthalene were quantified using qPCR with the method described earlier (d, $n = 6$). Transcript levels of metastatic markers, *cdh1* and *mmp9*, were quantified by qPCR at 1 and 3 dpt of naphthalene (e, $n = 4–8$; $0.01 < *p < 0.05$; $**p < 0.01$).

difference was found between these two groups ($p = 0.120$, Fig. 4d). The downregulation of *cdh1* expression in both 0.1 and 1 ppm naphthalene-treated cells was found at 1 dpt, showing 0.57 ± 0.07 (**$p = 0.001$) and 0.67 ± 0.09 (**$p = 0.006$) fold increase of the control cells (Fig. 4e), respectively. The regaining of the *cdh1* expression level was only observed in 0.1 ppm naphthalene-treated cells at 3 dpt, with a 6.50 ± 1.44 fold increase of the control cells (*$p = 0.011$, Fig. 4e). The upregulation of *mmp9* in naphthalene-treated cells was found as early as 1 dpt. The fold changes in 0.1 and 1 ppm naphthalene treated groups were 13.27 ± 2.33 and 11.04 ± 3.10, respectively, and both showed significant differences in comparison to the control group (Fig. 4e).

PFOA activated the AhR *in vitro* and *in vivo*

Aromatic hydrocarbons are a group of compounds that have long been identified as ligands of AhR.[50] As the two common PAH chemicals, anthracene and naphthalene are known to have different binding capabilities to AhR. Anthracene was considered an agonist of AhR, enhancing the AhR downstream pathways.[51] In contrast, naphthalene was believed to be an inactive ligand for AhR; however, metabolites of naphthalene in hepatocytes, such as 1,2-naphthoquinone and 1,4-naphthoquinone,[52] were found to be strong AhR ligands.[53] Therefore, the results of AhR activation in HepG2-LuciaTM AhR cells by the treatments of anthracene and naphthalene are similar in our study. Unlike the PAH family, the PFAS were arguably considered AhR ligands due to the lack of aromatic rings in their chemical structures. Perfluorooctane sulfonamide (PFOSA)[54,55] and 8 : 2 fluorotelomer alcohol (8 : 2 FTOH)[56] were reported to be bona fide AhR ligands. In addition, the PFDoA and PFDA also demonstrated activating effects on AhR as reported by Long *et al.*[57] Although Long's study showed no agonistic effects of PFOA on AhR,[57] a recent study suggested that PFOA induced heart maldevelopment in zebrafish embryos through AhR-mediated oxidative stress.[58] The results of our *in vitro* study confirmed the activation of AhR by the treatment of anthracene and naphthalene (Fig. 5a). All three concentrations of anthracene activate the production of luciferase *via* AhR, as shown by the relative light unit (RLU) from 173.5 ± 10.2 to 817.9 ± 65.9 (0.1 ppm, **$p = 0.002$), 707.6 ± 42.5 (1 ppm, *$p = 0.032$), and 1004.0 ± 86.8 (10 ppm, **$p < 0.0001$). Similarly, 0.1, 1, and 10 ppm of naphthalene treatment induced the luciferase to 851.6 ± 73.0 (**$p = 0.0004$), 880.6 ± 34.9 (**$p = 0.0007$), and 709.1 ± 41.9 ($p = 0.062$) RLUs, respectively. The activation of AhR in cells treated with anthracene and naphthalene was likely from both the original chemicals and metabolized products, including quinones (Fig. 5a). AhR activation in the HepG2-Lucia™ AhR cells was also achieved by the application of PFOA at concentrations of 0.1, 1, and 10 ppm, as they elevated the RLUs to 738.5 ± 51.4 (**$p = 0.0006$), 696.4 ± 50.5 (**$p = 0.0099$), and 767.9 ± 41.3 (**$p = 0.0006$), respectively. Although 10 ppm resulted in an RLU level to 644.0 ± 46.2, there was no significant difference compared to the control group ($p = 0.086$). We came up with a possible explanation for the activation of AhR by PFOA without an aromatic ring structure. Most of the PFAS chemicals,

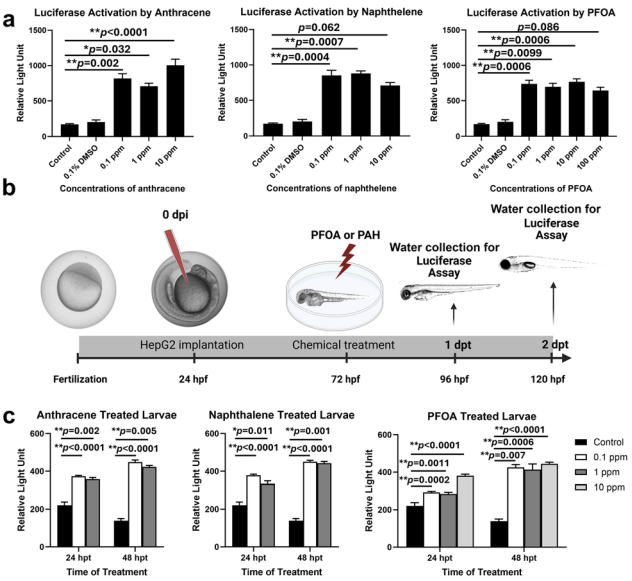

Fig. 5 Activation of the AhR pathway by PFOA *in vitro* and *in vivo*. The activities of secreted luciferase by HepG2-Lucia™ AhR cell cultures treated with various concentrations of anthracene, naphthalene, and PFOA were measured from the cell culture media (a, $n = 8$; 0.01 < *p < 0.05; **p < 0.01). The procedures for the luciferase *in vivo* assay are illustrated (b). The luciferase activities in the water of zebrafish larva holding wells were measured (c, $n = 10$; 0.01 < *p < 0.05; **p < 0.01).

including PFOA, were proven to be activators/ligands for peroxisome proliferator-activated receptors (PPARs), another family of nuclear receptors acting as transcription factors for gene expression.[59] Crosstalk between AhR and PPAR pathways has been identified in many organs, particularly in livers.[60–62] This crosstalk, which happened downstream of AhR, could potentially activate the expression of luciferase, resulting in a similar result as the activation of AhR.

The *in vitro* results were confirmed with the *in vivo* assay, which included a more complicated microenvironment for the cells. Because the luciferase produced by the HepG2-Lucia™ AhR cells was expected to be secreted, we expected to detect the luciferase activities in the water of each well (Fig. 5b). A similar study detecting the luciferase activities in the water holding a luciferase-based transgenic reporter zebrafish was previously documented.[63] The *in vivo* results of our study confirmed those from the *in vitro* assay. All concentrations of anthracene, naphthalene, and PFOA treatments resulted in increased luciferase production (Fig. 5c). This suggested that the PFOA activated the AhR pathway of the HepG2 cells *in vivo*, like the PAH compounds. Anthracene and naphthalene efficiently activated the AhR pathway as early as 24 hpt. In contrast, the AhR activation by PFOA appeared to be slower. Although a significant increase of luciferase in water was detected in the groups treated with the three concentrations of PFOA (0.1, 1, and 10 ppm) at 24 hpt, the levels of increase were marginal (292.5 ± 6.0, 284.6 ± 8.8, and 381.4 ± 7.8 RLUs, at 0.1, 1, and 10 ppm, respectively, Fig. 5c). At 48 hpt, the levels of secreted luciferase were further elevated by the treatment of all three

concentrations of PFOA, resulting in 425.8 ± 15.2, 413.1 ± 30.6, and 444.7 ± 8.55 RLUs at 0.1, 1, and 10 ppm, respectively (Fig. 5c).

Unlike anthracene and naphthalene, PFOA is believed to remain stable in humans and can hardly be metabolized by any type of human cell.[64] The half-lives of PFOA in serum elimination were reported to be 3.5–3.8 years.[65] In comparison, the half-lives of the PAHs range from hours to days.[66–68] Therefore, prolonged effects of PFOA on the AhR pathway in human cells are expected, although it is not clear whether the effect is caused by direct binding to the AhR or interactions with the PPAR pathway, which is believed to be the primary target of most PFAS chemicals.

Conclusions

The present study developed and optimized a zebrafish xenograft model using the human HepG2-Lucia™ AhR cell line to evaluate the carcinogenic effects of PFOA. This model was proven to be reliable in assessing the *in vivo* behaviors of HepG2 cells, such as migration, proliferation, and progression. PFOA was found to significantly induce the metastasis of HepG2 cells, including enhanced cell migration, significantly promoted cell migration, and elevation of metastatic cell markers. With the assistance of the model, we also investigated the possible mechanisms of PFOA-triggered hepatocyte carcinogenesis. Using the AhR luciferase reporting system in the HepG2-Lucia™ AhR cells, we identified the activation of the AhR pathway by PFOA, which was similar to the effects caused by the two PAH compounds, anthracene and naphthalene. Although the AhR activation by PFOA was difficult to explain based on the structure of PFOA and the previous studies, the indirect activation initiated by the crosstalk between AhR and PPARs, which are the primary targets of PFOA, was likely to be the carcinogenic mechanism of PFOA on hepatocytes. Further studies focusing on the interactions between AhR and PFOA-activated PPAR pathways are desired.

Author contributions

K. E. H. – data curation; formal analysis; investigation; validation; visualization; writing – original draft. E. K. – data curation; investigation; validation. G. B. – supervision; writing – review & editing. W. X. – conceptualization; data curation; formal analysis; funding acquisition; investigation; methodology; project administration; resources; supervision; visualization; writing – review & editing.

Conflicts of interest

There are no conflicts to declare.

Data availability

All data were included in the manuscript or the supplementary information (SI). Supplementary information: sequences for the qPCR primers used in this study (Table S1), data normal distribution tests (Shapiro–Wilk test) for all the data used for statistical analysis (Fig. S1–S3), and the standard curve for tumor cell *in vivo* quantification using the qPCR data for *tbp* gene (Fig. S4). See DOI: https://doi.org/10.1039/d5va00491h.

Acknowledgements

The authors would like to thank Dr Ramon Lavado from Baylor University for the HepG2-Lucia™ AhR cells. This study was supported by the Matagorda Bay Mitigation Trust grant.

References

1 J. Choi, J. Y. Kim and H. J. Lee, Human Evidence of Perfluorooctanoic Acid (PFOA) Exposure on Hepatic Disease: A Systematic Review and Meta-Analysis, *Int. J. Environ. Res. Publ. Health*, 2022, **19**(18), 11318.
2 K. Li, P. Gao, P. Xiang, X. Zhang, X. Cui and L. Q. Ma, Molecular mechanisms of PFOA-induced toxicity in animals and humans: Implications for health risks, *Environ. Int.*, 2017, **99**, 43–54.
3 M. E. Solan and R. Lavado, Effects of short-chain per- and polyfluoroalkyl substances (PFAS) on human cytochrome P450 (CYP450) enzymes and human hepatocytes: An *in vitro* study, *Curr. Res. Toxicol.*, 2023, **5**, 100116.
4 E. J. Sun, M. Wankell, P. Palamuthusingam, C. McFarlane and L. Hebbard, Targeting the PI3K/Akt/mTOR Pathway in Hepatocellular Carcinoma, *Biomedicines*, 2021, **9**(11), 1639.
5 F. Tonon, R. Farra, C. Zennaro, G. Pozzato, N. Truong, S. Parisi, F. Rizzolio, M. Grassi, B. Scaggiante, F. Zanconati, D. Bonazza, G. Grassi and B. Dapas, Xenograft Zebrafish Models for the Development of Novel Anti-Hepatocellular Carcinoma Molecules, *Pharmaceuticals*, 2021, **14**(8), 803.
6 G. Singh, S. Trehan, A. Singh, K. Goswami, A. Farooq, P. Antil, P. Puri, G. Bector, A. Jain and W. Azhar, Aryl Hydrocarbon Receptor Signaling in Prostate Cancer Therapy: A Review of Implications for Anti-androgen Treatment Strategies and Resistance, *Cureus*, 2024, **16**, e65247.
7 A. G. Singal, N. D. Parikh, N. E. Rich, B. V. John and A. Pillai, in *Hepatocellular Carcinoma: Translational Precision Medicine Approaches*, ed. Y. Hoshida, Cham (CH), 2019, pp. 27–51, DOI: 10.1007/978-3-030-21540-8_2.
8 R. Lencioni, J. Marrero, A. Venook, S. L. Ye and M. Kudo, Design and rationale for the non-interventional Global Investigation of Therapeutic DEcisions in Hepatocellular Carcinoma and Of its Treatment with Sorafenib (GIDEON) study, *Int. J. Clin. Pract.*, 2010, **64**, 1034–1041.
9 A. Gabrielson, A. A. Tesfaye, J. L. Marshall, M. J. Pishvaian, B. Smaglo, R. Jha, K. Dorsch-Vogel, H. Wang and A. R. He, Phase II study of temozolomide and veliparib combination therapy for sorafenib-refractory advanced hepatocellular carcinoma, *Cancer Chemother. Pharmacol.*, 2015, **76**, 1073–1079.
10 H. Rumgay, M. Arnold, J. Ferlay, O. Lesi, C. J. Cabasag, J. Vignat, M. Laversanne, K. A. McGlynn and

I. Soerjomataram, Global burden of primary liver cancer in 2020 and predictions to 2040, *J. Hepatol.*, 2022, **77**, 1598–1606.

11 S. Qiu, J. Cai, Z. Yang, X. He, Z. Xing, J. Zu, E. Xie, L. Henry, C. R. Chong, E. M. John, R. Cheung, F. Ji and M. H. Nguyen, Trends in Hepatocellular Carcinoma Mortality Rates in the US and Projections Through 2040, *JAMA Netw. Open*, 2024, **7**, e2445525.

12 H. Samant, H. S. Amiri and G. B. Zibari, Addressing the worldwide hepatocellular carcinoma: epidemiology, prevention and management, *J. Gastrointest. Oncol.*, 2021, **12**, S361–S373.

13 Y. Hong, D. Wang, Z. Liu, Y. Chen, Y. Wang and J. Li, Decoding per- and polyfluoroalkyl substances (PFAS) in hepatocellular carcinoma: a multi-omics and computational toxicology approach, *J. Transl. Med.*, 2025, **23**, 504.

14 D. Y. Stainier, B. Fouquet, J. N. Chen, K. S. Warren, B. M. Weinstein, S. E. Meiler, M. A. Mohideen, S. C. Neuhauss, L. Solnica-Krezel, A. F. Schier, F. Zwartkruis, D. L. Stemple, J. Malicki, W. Driever and M. C. Fishman, Mutations affecting the formation and function of the cardiovascular system in the zebrafish embryo, *Development*, 1996, **123**, 285–292.

15 N. Shimizu, H. Shiraishi and T. Hanada, Zebrafish as a Useful Model System for Human Liver Disease, *Cells*, 2023, **12**(18), 2246.

16 C. Tulotta, S. He, L. Chen, A. Groenewoud, W. van der Ent, A. H. Meijer, H. P. Spaink and B. E. Snaar-Jagalska, Imaging of Human Cancer Cell Proliferation, Invasion, and Micrometastasis in a Zebrafish Xenogeneic Engraftment Model, *Methods Mol. Biol.*, 2016, **1451**, 155–169.

17 M. Adhish and I. Manjubala, Effectiveness of zebrafish models in understanding human diseases-A review of models, *Heliyon*, 2023, **9**, e14557.

18 C. Huang, I. Murgulet, L. Liu, M. Zhang, K. Garcia, L. Martin and W. Xu, The effects of perfluorooctanoic acid on breast cancer metastasis depend on the phenotypes of the cancer cells: An *in vivo* study with zebrafish xenograft model, *Environ. Pollut.*, 2024, **362**, 124975.

19 W. Xu, B. A. Foster, M. Richards, K. R. Bondioli, G. Shah and C. C. Green, Characterization of prostate cancer cell progression in zebrafish xenograft model, *Int. J. Oncol.*, 2018, **52**, 252–260.

20 F. N. David and N. L. Johnson, The effect of non-normality on the power function of the F-test in the analysis of variance, *Biometrika*, 1951, **38**, 43–57.

21 W. H. Kruskal and W. A. Wallis, Use of Ranks in One-Criterion Variance Analysis, *J. Am. Stat. Assoc.*, 1952, **47**, 583–621.

22 O. J. Dunn, Multiple Comparisons Using Rank Sums, *Technometrics*, 1964, **6**, 241.

23 J. F. De la Paz, C. Anguita-Salinas, C. Diaz-Celis, F. P. Chavez and M. L. Allende, The Zebrafish Perivitelline Fluid Provides Maternally-Inherited Defensive Immunity, *Biomolecules*, 2020, **10**(9), 1274.

24 B. A. Lewis, P. M. Lokman and C. W. Beck, A Novel Approach to Perivitelline Fluid Extraction from Live Water-Activated Eggs from Zebrafish, *Fishes*, 2025, **10**(8), 369.

25 S. Zahm, J. P. Bonde, W. A. Chiu, J. Hoppin, J. Kanno, M. Abdallah, C. R. Blystone, M. M. Calkins, G. H. Dong, D. C. Dorman, R. Fry, H. Guo, L. S. Haug, J. N. Hofmann, M. Iwasaki, M. Machala, F. R. Mancini, S. S. Maria-Engler, P. Moller, J. C. Ng, M. Pallardy, G. B. Post, S. Salihovic, J. Schlezinger, A. Soshilov, K. Steenland, I. L. Steffensen, V. Tryndyak, A. White, S. Woskie, T. Fletcher, A. Ahmadi, N. Ahmadi, L. Benbrahim-Tallaa, W. Bijoux, S. Chittiboyina, A. de Conti, C. Facchin, F. Madia, H. Mattock, M. Merdas, E. Pasqual, E. Suonio, S. Viegas, L. Zupunski, R. Wedekind and M. K. Schubauer-Berigan, Carcinogenicity of perfluorooctanoic acid and perfluorooctanesulfonic acid, *Lancet Oncol.*, 2024, **25**, 16–17.

26 USEPA, *Human Health Toxicity Assessment for Perfluorooctanoic Acid (PFOA) and Related Salts*, Washington, DC, 2024.

27 P. K. Gupta, in *Fundamentals of Toxicology*, ed. P. K. Gupta, Academic Press, 2016, pp. 23–29, DOI: 10.1016/B978-0-12-805426-0.00004-4.

28 E. E. Rosowski, Determining macrophage *versus* neutrophil contributions to innate immunity using larval zebrafish, *Dis. Model. Mech.*, 2020, **13**(1), dmm041889.

29 M. Hashiguchi, S. Ueno, M. Sakoda, S. Iino, K. Hiwatashi, K. Minami, K. Ando, Y. Mataki, K. Maemura, H. Shinchi, S. Ishigami and S. Natsugoe, Clinical implication of ZEB-1 and E-cadherin expression in hepatocellular carcinoma (HCC), *BMC Cancer*, 2013, **13**, 572.

30 T. Matsumura, R. Makino and K. Mitamura, Frequent down-regulation of E-cadherin by genetic and epigenetic changes in the malignant progression of hepatocellular carcinomas, *Clin. Cancer Res.*, 2001, **7**, 594–599.

31 A. M. Mendonsa, T. Y. Na and B. M. Gumbiner, E-cadherin in contact inhibition and cancer, *Oncogene*, 2018, **37**, 4769–4780.

32 J. Yang and R. A. Weinberg, Epithelial-mesenchymal transition: at the crossroads of development and tumor metastasis, *Dev. Cell*, 2008, **14**, 818–829.

33 G. Berx and F. van Roy, Involvement of members of the cadherin superfamily in cancer, *Cold Spring Harbor Perspect. Biol.*, 2009, **1**, a003129.

34 H. Huang, Matrix Metalloproteinase-9 (MMP-9) as a Cancer Biomarker and MMP-9 Biosensors: Recent Advances, *Sensors*, 2018, **18**(10), 3249.

35 Y. Xu, H. Tian, C. G. Luan, K. Sun, P. J. Bao, H. Y. Zhang and N. Zhang, Telocytes promote hepatocellular carcinoma by activating the ERK signaling pathway and miR-942-3p/MMP9 axis, *Cell Death Discov.*, 2021, **7**, 209.

36 J. R. Kim and C. H. Kim, Association of a high activity of matrix metalloproteinase-9 to low levels of tissue inhibitors of metalloproteinase-1 and -3 in human hepatitis B-viral hepatoma cells, *Int. J. Biochem. Cell Biol.*, 2004, **36**, 2293–2306.

37 C. Sweeney, G. Lazennec and C. F. A. Vogel, Environmental exposure and the role of AhR in the tumor

microenvironment of breast cancer, *Front. Pharmacol*, 2022, **13**, 1095289.

38 C. E. Bostrom, P. Gerde, A. Hanberg, B. Jernstrom, C. Johansson, T. Kyrklund, A. Rannug, M. Tornqvist, K. Victorin and R. Westerholm, Cancer risk assessment, indicators, and guidelines for polycyclic aromatic hydrocarbons in the ambient air, *Environ. Health Perspect.*, 2002, **110**(3), 451–488.

39 S. Y. Eom, D. H. Yim, S. I. Moon, J. W. Youn, H. J. Kwon, H. C. Oh, J. J. Yang, S. K. Park, K. Y. Yoo, H. S. Kim, K. S. Lee, S. H. Chang, Y. D. Kim, J. W. Kang and H. Kim, Polycyclic aromatic hydrocarbon-induced oxidative stress, antioxidant capacity, and the risk of lung cancer: a pilot nested case-control study, *Anticancer Res.*, 2013, **33**, 3089–3097.

40 Y. Ni, W. Wang, Y. Xu and W. Zhang, A study on the impact of polycyclic aromatic hydrocarbons (PAHs) on the risk of liver disease in middle-aged and older adults people based on the CHARLS database, *Ecotoxicol. Environ. Saf.*, 2025, **300**, 118493.

41 M. S. Volkov, N. A. Bolotina, V. A. Evteev and V. A. Koblyakov, Ah-receptor-independent stimulation of hepatoma 27 culture cell proliferation by polycyclic aromatic hydrocarbons, *Biochemistry*, 2012, **77**, 201–207.

42 B. A. Rybicki, N. L. Nock, A. T. Savera, D. Tang and A. Rundle, Polycyclic aromatic hydrocarbon-DNA adduct formation in prostate carcinogenesis, *Cancer Lett.*, 2006, **239**, 157–167.

43 E. Hruba, J. Vondracek, H. Libalova, J. Topinka, V. Bryja, K. Soucek and M. Machala, Gene expression changes in human prostate carcinoma cells exposed to genotoxic and nongenotoxic aryl hydrocarbon receptor ligands, *Toxicol. Lett.*, 2011, **206**, 178–188.

44 A. Jurisicova, A. Taniuchi, H. Li, Y. Shang, M. Antenos, J. Detmar, J. Xu, T. Matikainen, A. Benito Hernandez, G. Nunez and R. F. Casper, Maternal exposure to polycyclic aromatic hydrocarbons diminishes murine ovarian reserve *via* induction of Harakiri, *J. Clin. Invest.*, 2007, **117**, 3971–3978.

45 A. Rafiee, M. Hoseini, S. Akbari and E. M. Mahabee-Gittens, Exposure to Polycyclic Aromatic Hydrocarbons and adverse reproductive outcomes in women: current status and future perspectives, *Rev. Environ. Health*, 2024, **39**, 305–311.

46 M. L. Perepechaeva and A. Y. Grishanova, The Role of Aryl Hydrocarbon Receptor (AhR) in Brain Tumors, *Int. J. Mol. Sci.*, 2020, **21**(8), 2863.

47 Y. Shimizu, Y. Nakatsuru, M. Ichinose, Y. Takahashi, H. Kume, J. Mimura, Y. Fujii-Kuriyama and T. Ishikawa, Benzo[a]pyrene carcinogenicity is lost in mice lacking the aryl hydrocarbon receptor, *Proc. Natl. Acad. Sci. U. S. A.*, 2000, **97**, 779–782.

48 S. Shi, D. Y. Yoon, K. C. Hodge-Bell, I. G. Bebenek, M. J. Whitekus, R. Zhang, A. J. Cochran, S. Huerta-Yepez, S. H. Yim, F. J. Gonzalez, A. K. Jaiswal and O. Hankinson, The aryl hydrocarbon receptor nuclear translocator (Arnt) is required for tumor initiation by benzo[a]pyrene, *Carcinogenesis*, 2009, **30**, 1957–1961.

49 C. Vogeley, K. M. Rolfes, J. Krutmann and T. Haarmann-Stemmann, The Aryl Hydrocarbon Receptor in the Pathogenesis of Environmentally-Induced Squamous Cell Carcinomas of the Skin, *Front. Oncol.*, 2022, **12**, 841721.

50 L. Lin, Y. Dai and Y. Xia, An overview of aryl hydrocarbon receptor ligands in the Last two decades (2002-2022): A medicinal chemistry perspective, *Eur. J. Med. Chem.*, 2022, **244**, 114845.

51 P. B. Busbee, M. Rouse, M. Nagarkatti and P. S. Nagarkatti, Use of natural AhR ligands as potential therapeutic modalities against inflammatory disorders, *Nutr. Rev.*, 2013, **71**, 353–369.

52 A. S. Wilson, C. D. Davis, D. P. Williams, A. R. Buckpitt, M. Pirmohamed and B. K. Park, Characterisation of the toxic metabolite(s) of naphthalene, *Toxicology*, 1996, **114**, 233–242.

53 Y. Cheng, U. H. Jin, L. A. Davidson, R. S. Chapkin, A. Jayaraman, P. Tamamis, A. Orr, C. Allred, M. S. Denison, A. Soshilov, E. Weaver and S. Safe, Editor's Highlight: Microbial-Derived 1,4-Dihydroxy-2-naphthoic Acid and Related Compounds as Aryl Hydrocarbon Receptor Agonists/Antagonists: Structure-Activity Relationships and Receptor Modeling, *Toxicol. Sci.*, 2017, **155**, 458–473.

54 H. Chen, W. Qiu, X. Yang, F. Chen, J. Chen, L. Tang, H. Zhong, J. T. Magnuson, C. Zheng and E. G. Xu, Perfluorooctane Sulfonamide (PFOSA) Induces Cardiotoxicity *via* Aryl Hydrocarbon Receptor Activation in Zebrafish, *Environ. Sci. Technol.*, 2022, **56**, 8438–8448.

55 P. Chen, K. Wang, J. Zhang, Y. Jiang and T. Chen, The Aryl Hydrocarbon Receptor Mediates the Neurodevelopmental Toxicity of Perfluorooctane Sulfonamide in Zebrafish Larvae, *Toxics*, 2025, **13**(10), 832.

56 M. Chen, J. H. Xu, Z. Chen, Z. W. Liang, C. Peng, D. M. Chen and S. Y. Xie, 8:2 fluorotelomer alcohol exacerbates doxorubicin-induced cardiotoxicity and chemoresistance *via* aryl hydrocarbon receptor, *Ecotoxicol. Environ. Saf.*, 2025, **303**, 118766.

57 M. Long, M. Ghisari and E. C. Bonefeld-Jorgensen, Effects of perfluoroalkyl acids on the function of the thyroid hormone and the aryl hydrocarbon receptor, *Environ. Sci. Pollut. Res. Int.*, 2013, **20**, 8045–8056.

58 X. Chen, T. Ma, K. Wang, T. Chen and Y. Jiang, Perfluorooctanoic acid induces abnormal heart development *via* aryl hydrocarbon receptor-mediated oxidative stress and apoptosis in zebrafish larvae, *J. Environ. Occup. Med.*, 2024, **41**, 1354–1360.

59 I. Issemann and S. Green, Activation of a member of the steroid hormone receptor superfamily by peroxisome proliferators, *Nature*, 1990, **347**, 645–650.

60 S. Gui, H. Pu, Y. Chen, Z. Liao, J. Liu and R. Fan, AhR/PPARgamma mediates hepatic lipid metabolism disorders induced by exposure to 16 priority-controlled PAHs at environment related doses, *Environ. Pollut.*, 2026, **388**, 127360.

61 T. S. Sayed, Z. H. Maayah, H. A. Zeidan, A. Agouni and H. M. Korashy, Insight into the physiological and

pathological roles of the aryl hydrocarbon receptor pathway in glucose homeostasis, insulin resistance, and diabetes development, *Cell. Mol. Biol. Lett.*, 2022, **27**, 103.

62 H. Dou, Y. Duan, X. Zhang, Q. Yu, Q. Di, Y. Song, P. Li and Y. Gong, Aryl hydrocarbon receptor (AhR) regulates adipocyte differentiation by assembling CRL4B ubiquitin ligase to target PPARgamma for proteasomal degradation, *J. Biol. Chem.*, 2019, **294**, 18504–18515.

63 J. R. Becker, T. Y. Robinson, C. Sachidanandan, A. E. Kelly, S. Coy, R. T. Peterson and C. A. MacRae, In vivo natriuretic peptide reporter assay identifies chemical modifiers of hypertrophic cardiomyopathy signalling, *Cardiovasc. Res.*, 2012, **93**, 463–470.

64 K. Steenland, T. Fletcher and D. A. Savitz, Epidemiologic evidence on the health effects of perfluorooctanoic acid (PFOA), *Environ. Health Perspect.*, 2010, **118**, 1100–1108.

65 G. W. Olsen, J. M. Burris, D. J. Ehresman, J. W. Froehlich, A. M. Seacat, J. L. Butenhoff and L. R. Zobel, Half-life of serum elimination of perfluorooctanesulfonate,perfluorohexanesulfonate, and perfluorooctanoate in retired fluorochemical production workers, *Environ. Health Perspect.*, 2007, **115**, 1298–1305.

66 Z. Li, L. Romanoff, S. Bartell, E. N. Pittman, D. A. Trinidad, M. McClean, T. F. Webster and A. Sjodin, Excretion profiles and half-lives of ten urinary polycyclic aromatic hydrocarbon metabolites after dietary exposure, *Chem. Res. Toxicol.*, 2012, **25**, 1452–1461.

67 O. Motorykin, L. Santiago-Delgado, D. Rohlman, J. E. Schrlau, B. Harper, S. Harris, A. Harding, M. L. Kile and S. L. Massey Simonich, Metabolism and excretion rates of parent and hydroxy-PAHs in urine collected after consumption of traditionally smoked salmon for Native American volunteers, *Sci. Total Environ.*, 2015, **514**, 170–177.

68 S. Shahin, A. Ghassabian, S. M. Blaauwendraad, C. Duh-Leong, K. Kannan, S. E. Long, T. Herrera, E. Seok, K. A. Pierce, M. Liu and L. Trasande, Prenatal polycyclic aromatic hydrocarbons exposure and child growth and adiposity: A longitudinal study, *Environ. Res.*, 2025, **268**, 120756.